Effect of the number of stacking layers on the characteristics of quantum-dash lasers

Effect of the number of stacking layers on the characteristics of quantum-dash lasers

M. Z. M. Khan,[1] T. K. Ng,[1] U. Schwingenschlogl,[1] P. Bhattacharya,[2] and B. S. Ooi[1,*]

[1]*Division of Physical Sciences and Engineering, King Abdullah University of Science & Technology (KAUST), Thuwal 23955-6900, Saudi Arabia.*

[2]*Department of Electrical Engineering and Computer Science, University of Michigan, 1301, Beal Avenue, Ann Arbor, Michigan 48109-2122, USA*

**boon.ooi@kaust.edu.sa*

Abstract: A theoretical model is evaluated to investigate the characteristics of InAs/InP quantum dash (Qdash) lasers as a function of the stack number. The model is based on multimode carrier-photon rate equations and accounts for both inhomogeneous and homogeneous broadenings of the optical gain. The numerical results show a non monotonic increase in the threshold current density and a red shift in the lasing wavelength on increasing the stack number, which agrees well with reported experimental results. This observation may partly be attributed to an increase of inhomogeneity in the active region.

OCIS codes: (140.5960) Semiconductor lasers; (250.5590) Quantum-well, -wire and -dot devices.

References and links

1. F. Lelarge, B. Dagens, J. Renaudier, R. Brenot, A. Accard, F. van Dijk, D. Make, O. Le Gouezigou, J. Provost, and F. Poingt, "Recent advances on InAs/InP quantum dash based semiconductor lasers and optical amplifiers operating at 1.55 m," IEEE J. Sel. Top. Quantum Electron. **13**(1), 111–124 (2007).
2. J. Reithmaier, A. Somers, S. Deubert, R. Schwertberger, W. Kaiser, A. Forchel, M. Calligaro, P. Resneau, O. Parillaud, S. Bansropun, M. Krakowski, R. Alizon, D. Hadass, A. Bilenca, H. Dery, V. Mikhelashvili, G. Eisenstein, M. Gioannini, I. Montrosset, T. W. Berg, M. Poel, J. Mørk, and B. Tromborg, "InP based lasers and optical amplifiers with wire-/dot-like active regions," J. Phys. D Appl. Phys. **38**(13), 2088–2102 (2005).
3. C. Tan, H. Djie, Y. Wang, C. Dimas, V. Hongpinyo, Y. Ding, and B. Ooi, "Wavelength tuning and emission width widening of ultrabroad quantum dash interband laser," Appl. Phys. Lett. **93**(11), 111101 (2008).
4. D. Zhou, R. Piron, M. Dontabactouny, O. Dehaese, F. Grillot, T. Batte, K. Tavernier, J. Even, and S. Loualiche, "Low threshold current density of InAs quantum dash laser on InP (100) through optimizing double cap technique," Appl. Phys. Lett. **94**(8), 081107 (2009).
5. D. Zhou, R. Piron, M. Dontabactouny, E. Homeyer, O. Dehaese, T. Batte, M. Gicquel, F. Grillot, K. Tavernier, J. Even, and S. Loualiche, "Effect of stack number on the threshold current density and emission wavelength in quantum dash/dot lasers," Phys. Status Solidi **6**(10), 2217–2221 (2009) (c).
6. D. Zhou, R. Piron, F. Grillot, O. Dehaese, E. Homeyer, M. Dontabactouny, T. Batte, K. Tavernier, J. Even, and S. Loualiche, "Study of the characteristics of 1.55 m quantum dash/dot semiconductor lasers on InP substrate," Appl. Phys. Lett. **93**(16), 161104 (2008).
7. C. Tan, H. Djie, Y. Wang, C. Dimas, V. Hongpinyo, Y. Ding, and B. Ooi, "The influence of nonequilibrium distribution on room-temperature lasing spectra in quantum-dash lasers," IEEE Photon. Technol. Lett. **21**(1), 30–32 (2009).
8. M. Gioannini, "Numerical modeling of the emission characteristics of semiconductor quantum dash materials for lasers and optical amplifiers," IEEE J. Quantum Electron. **40**(4), 364–373 (2004).
9. Z. Mi, and P. Bhattacharya, "DC and dynamic characteristics of P-doped and tunnel injection 1.65- m InAs quantum-dash lasers grown on InP (001)," IEEE J. Quantum Electron. **42**(11–12), 1224–1232 (2006).
10. H. Dery, and G. Eisenstein, "Self-consistent rate equations of self-assembly quantum wire lasers," IEEE J. Quantum Electron. **40**(10), 1398–1409 (2004).
11. M. Sugawara, K. Mukai, Y. Nakata, H. Ishikawa, and A. Sakamoto, "Effect of homogeneous broadening of optical gain on lasing spectra in self-assembled In_ {x} Ga_ {1-x} As/GaAs quantum dot lasers," Phys. Rev. B **61**(11), 7595–7603 (2000).
12. K. Veselinov, F. Grillot, C. Cornet, J. Even, A. Bekiarski, M. Gioannini, and S. Loualiche, "Analysis of the double laser emission occurring in 1.55- μm InAs–InP (113) B quantum-dot Lasers," IEEE J. Quantum Electron. **43**(9), 810–816 (2007).
13. F. Grillot, K. Veselinov, M. Gioannini, I. Montrosset, J. Even, R. Piron, E. Homeyer, and S. Loualiche, "Spectral analysis of 1.55 μm InAs–InP (113) B quantum-dot lasers based on a multipopulation rate equations model," IEEE J. Quantum Electron. **45**(7), 872–878 (2009).

#143370 - $15.00 USD Received 1 Mar 2011; revised 12 May 2011; accepted 17 May 2011; published 27 Jun 2011

14. D. Hadass, A. Bilenca, R. Alizon, H. Dery, V. Mikhelashvili, G. Eisenstein, R. Schwertberger, A. Somers, J. Reithmaier, A. Forchel, M. Calligaro, S. Bansropun, and M. Krakowski, "Gain and noise saturation of wide-band InAs-InP quantum dash optical amplifiers: model and experiments," IEEE J. Sel. Top. Quantum Electron. **11**(5), 1015–1026 (2005).
15. R. Schwertberger, D. Gold, J. Reithmaier, and A. Forchel, "Long-wavelength InP-based quantum-dash lasers," IEEE Photon. Technol. Lett. **14**(6), 735–737 (2002).
16. T. Amano, S. Aoki, T. Sugaya, K. Komori, and Y. Okada, "Laser characteristics of 1.3-μm quantum dots laser with high-density quantum dots," IEEE J. Sel. Top. Quantum Electron. **13**(5), 1273–1278 (2007).
17. N. Nuntawong, Y. Xin, S. Birudavolu, P. Wong, S. Huang, C. Hains, and D. Huffaker, "Quantum dot lasers based on a stacked and strain-compensated active region grown by metal-organic chemical vapor deposition," Appl. Phys. Lett. **86**(19), 193115 (2005).
18. L. Asryan, and R. Suris, "Inhomogeneous line broadening and the threshold current density of a semiconductor quantum dot laser," Semicond. Sci. Technol. **11**(4), 554–567 (1996).

1. Introduction

Tuning the emission wavelength of Qdash and quantum dot (Qdot) lasers depends primarily on the size of the nano structures and particularly the height [1,2]. This feature together with the InP technology and various process techniques has enabled the demonstration of Qdash/Qdot lasers in the c-band telecommunication window with improved performances [3,4]. On the other hand, recent experimental studies on InAs/InP Qdash lasers by different research groups have reported the dependence of the lasing wavelength on laser structural parameters [5–7]. They have observed a red shift in the lasing wavelength on increasing the number of stack layers or the cavity length. This observation is ascribed to the unique characteristics of Qdashes determined by their density of states (DOS), in general [5,7]. However, the phenomenon needs more physical insight, particularly the stacking layer effect as this is a fundamental technique to improve the characteristics of Qdash lasers. Therefore, a theoretical assessment is essential to understand the phenomenon in a more comprehensive manner. In addition, one may expect this observation as a result of alteration to other laser parameters that change with the stack number. Our results are important as this is directly related to the spectral characteristics and, in general, the performance characteristics of the device.

In this work, a simulation model is considered to compare the characteristics of InAs/InP Qdash lasers as a function of the number of stacking layers. We theoretically verify the red shift in the central lasing wavelength (calculated by identifying the central wavelength at full width at half maximum (FWHM) of the lasing spectra) and non monotonic increase in the threshold current density on increasing the stack number. The numerical simulations show a good agreement with experimental observations. By the simulations we find that the phenomenon is partly due to the inherent change in the laser parameters particularly the active region inhomogeneity.

2. Theoretical model

The numerical model, applicable to InAs/InP Qdash lasers, is evaluated from the basic coupled rate equations of each Qdash ensemble incorporating the carrier and photon dynamics at each energy level. The technique is based on the density matrix formulation of the Qdash gain media [8,9] where the quantum wire like nature has a large influence on the gain properties of the laser [10]. The formulation is similar to the one reported for the analysis of both InGaAs/GaAs [11] and InAs/InP [12,13] Qdot lasers, and InAs/InP Qdash semiconductor optical amplifier [14], following identical assumptions. The dashes are grouped into $2M_d+1$ groups according to their central transition wavelength E_{cv} ($j=M_d$ corresponds to E_{cv}) and a series of longitudinal cavity photon modes ($m=0,1,..,2M_p$ modes with separation $\Delta E_m = ch/2n_aL$) are considered over the central photon mode energy E_{cvp} to describe the interaction between the dashes with different resonant energies and the generated photons. Furthermore, a single ground state (GS) with N intra-dash energy levels is considered in each dash ensemble characterized by the DOS function $N_D = N_{dh}\sqrt{2m_e^*/\pi^2\hbar^2}\sqrt{E_{j,N+1}-E_{j,0}}$ [14]. $E_{j,0}$

#143370 - $15.00 USD Received 1 Mar 2011; revised 12 May 2011; accepted 17 May 2011; published 27 Jun 2011

and $E_{j,N}$ correspond to the lowest and highest GS energy of the j^{th} dash group and $E_{j,k}$ represents a generic energy level of the system. We consider a three level energy system [11] consisting of the separate confinement heterostructure (SCH), the wetting layer (WL) and the GS energy levels of the dashes with carrier populations N_S, N_W and $N_{j,k}$, respectively. Both, the homogeneous Lorentzian broadening $B(E_m - E_{j,k})$ with FWHM $\hbar\Gamma_{hom}$ and inhomogeneous Gaussian broadening, of the optical gain is considered in the formulation. Therefore, the fraction of energy states available at the energy level $E_{j,k}$ is given by [14]:

$$G_{j,k} = \frac{1}{\sqrt{2\pi}\xi_0}\exp\left(\frac{\left(E_{j,0}-E_{cv}\right)^2}{2\xi_0^2}\right)dE_j\,\frac{\sqrt{E_{j,k+1}-E_{j,0}}-\sqrt{E_{j,k}-E_{j,0}}}{\sqrt{E_{j,N+1}-E_{j,0}}}. \tag{1}$$

The first term of Eq. (1) is the inhomogeneous term with FWHM of $\Gamma_{inh} = 2.35\xi_0$, while the second term is the ratio of two integrals [14]. Note that $G_{j,k}$ is normalized as $\sum_{j,k} G_{j,k} = 1$. The rate equations are as follows:

$$\frac{dN_S}{dt} = \frac{\eta_i I}{e} - \frac{N_S}{\tau_{SW}} - \frac{N_S}{\tau_S} + \frac{N_W}{\tau_{WS}}, \tag{2}$$

$$\frac{dN_W}{dt} = \frac{N_S}{\tau_{SW}} + \sum_j\sum_k \frac{N_{j,k}}{\tau_{DW}^{j,k}} - \frac{N_W}{\overline{\tau_{WD}}} - \frac{N_W}{\tau_{WS}} - \frac{N_W}{\tau_W}, \tag{3}$$

$$\frac{dN_{j,k}}{dt} = \frac{N_W G_{j,k}}{\tau_{WD}^{j,k}} - \frac{N_{j,k}}{\tau_{DW}^{j,k}} - \frac{N_W}{\tau_D} - \frac{c\Gamma}{n_a}\sum_m g_m^{j,k} S_m, \tag{4}$$

$$\frac{dS_m}{dt} = \beta\sum_k\sum_j B\left(E_m - E_{j,k}\right)\frac{N_{j,k}}{\tau_{Sp}} + \frac{c\Gamma}{n_a}\sum_k\sum_j g_m^{j,k} S_m - \frac{S_m}{\tau_p}. \tag{5}$$

Equations (2), (3) and (4) refer to the carrier dynamics in the SCH, WL and dash GS energy levels. *I* is the current injection, η_i is the internal quantum efficiency, $\tau_S(\tau_W, \tau_D)$ is the recombination lifetime in the SCH (WL,GS) layers, $\tau_{SW}(\overline{\tau_{WD}}, \tau_{WD}^{j,k})$ is the carrier relaxation lifetime from SCH(WL) to WL(GS) with the bar denoting an average lifetime [11,14], $\tau_{WS}(\tau_{DW})$ is the excitation lifetime from WL(GS) to SCH(WL), and τ_{Sp}, τ_p are the lifetimes of spontaneous emission and photons, respectively [11]. Note that τ_{DW} is calculated through the condition of detailed balance [14] and τ_p according to [11]. The multi-mode photon rate equation is given by Eq. (5) where S_m is the photon population of the m^{th} mode. Moreover,

$$g_m^{j,k} = \frac{2\pi e^2 \hbar N_D}{c n_a \epsilon_0 m_0^2}\frac{\left|M_{cv}\right|^2}{E_{cv}}\left(2P_{j,k}-1\right)G_{j,k}B\left(E_m - E_{j,k}\right) \tag{6}$$

represents the linear optical gain [8,9] of the $E_{j,k}$ dash group contributing to the m^{th} mode photons, where $\left|M_{cv}\right|^2$ is the transition matrix and $P_{j,k} = N_{j,k}/2D_g N_D V_A G_{j,k}$ is the carrier occupational probability (including the spin) [11,14].

#143370 - $15.00 USD Received 1 Mar 2011; revised 12 May 2011; accepted 17 May 2011; published 27 Jun 2011

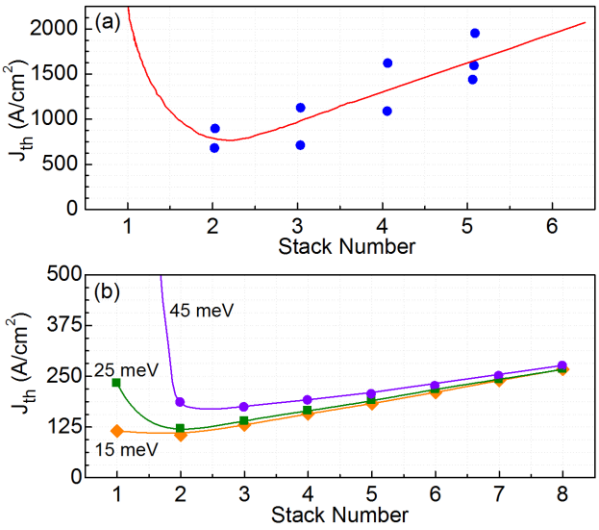

Fig. 1. (a) Experimental [5,6] and (b) Calculated threshold current density versus the number of stacking layers for the Qdash lasers reported in [5] and [15], respectively. The three curves in (b) correspond to various inhomogeneous broadening values.

The Qdash laser considered for the analysis is obtained from [15] and is based on the InAs/InP material system. Four stacks of InAs Qdashes with an average height of 1.5 *nm* and width of 20 *nm* constitutes the active region with volume $V_A = 1.8\times10^{16}\ cm^3$ and refractive index $n_a = 3.5$. The WL is 1 *nm* thick with a cross section dash density of $1.0\times10^{12}\ cm^{-2}$. The $L = 1.0\ mm$ long laser with $40\ \mu m$ stripe width has an internal loss of $\alpha_i = 10\ cm^{-1}$ and as-cleaved facets ($R_1 = R_2 = 0.3$) resulting in an optical loss of $\alpha_m \approx 12\ cm^{-1}$ [14,15].

The steady state lasing spectra are calculated [11] using the above set of rate equations with the fourth-order Runge-Kutta numerical method. We adopt an initial carrier relaxation lifetime of $\tau_{WD0} = 2\ ps$ from WL to dash GS, while the carrier relaxation to and re-excitation from SCH are $\tau_{SW} = 0.5\ ns$ and $\tau_{WS} = 1.0\ ns$, respectively. The recombination lifetimes within SCH, WL and Qdash GS are, respectively, $\tau_S = \infty$, $\tau_W = 0.8\ ns$ and $\tau_D = 0.5\ ns$ [14].

The degeneracies of the WL and GS is taken as $D_W = 1.8\times10^{19}\ cm^{-3}$ and $D_G = 1$, respectively, and the volumetric DOS is $N_D = 5\times10^{17}\ cm^{-3}$ [14]. The other parameters used in the model are [11,14]: $E_{cv} = 805\ meV$, energy level of WL $E_{WL} = 916\ meV$, $\hbar\Gamma_{hom} = 10\ meV$, optical confinement factor $\Gamma = 0.03$, spontaneous emission efficiency $\beta = 10^{-4}$ and lifetime $\tau_{sp} = 2.8\ ns$. The separation between the dash groups is $\Delta E_j = 0.354\ meV$, and $2M_d + 1$ varies from 201 to 401 based on the convergence achieved at each Γ_{inh} value once stabilizing the lasing spectrum.

3. Numerical results

Figure 1 illustrates the effect of the number of stacking layers (N_{lyr}) on the threshold current density (J_{th}) of Qdash lasers. The experimental data is obtained from [5,6] and is plotted in Fig. 1(a) for comparison. Figure 1(b) corresponds to the simulation results at various values of the inhomogeneous broadening (Γ_{inh}). A non monotonic increase in the threshold current density is observed on increasing the stack number, which is in good agreement with the experimental data except that the threshold current density values are different in Figs. 1(a)

#143370 - $15.00 USD Received 1 Mar 2011; revised 12 May 2011; accepted 17 May 2011; published 27 Jun 2011

and (b). This is an anticipated discrepancy owing to the fact that the two laser structures considered are rather different. Our aim here is to numerically address the trend of J_{th} and the central lasing wavelength (λ_c) as a function of the number of stacking layers and explain the behavior qualitatively. Therefore, we model the dash DOS high energy tail by a stair case approximation utilizing Eq. (1) with N = 50 rather than calculating the accurate energy states of the Qdashes. An almost linear increase in J_{th} is seen when $N_{lyr} > 2$ as show in Fig. 1(b), at all inhomogeneity values. This may be attributed to the active region volume V_A, the optical confinement factor Γ, and the inhomogeneous broadening. Increase in V_A due to stacking of the dash layers may enhance internal absorptions, thus affecting the threshold current density. On the other hand, a lower Γ (due to increase in V_A as a result of increase in N_{lyr}) probably assists in attaining the modal gain (Γg_{th}) relatively fast, thereby decreasing the threshold current density [6,16]. However, the results show an increase in J_{th} for $N_{lyr} > 2$ which suggests that V_A dominates. Moreover, increase in J_{th} could be due to an increase in modal gain as a result of stacking of the dash layers which has been reported experimentally [1,5,16]. Nevertheless, our model considers a fixed modal gain ($\Gamma g_{th} = \alpha_i + \alpha_m \approx 22\ cm^{-1}$) independent of the number of stacking layers in spite of varying Γ accordingly (0.009 per layer) and therefore, probably, does not affect the threshold current density numerically.

Increase in J_{th} due to N_{lyr} has also been attributed to the increase in Γ_{inh} by various experimental work as a result of change in dash sizes and density due to subsequent growth of dash layers [1,16,17]. However, in our analysis we assume an identical dash density per layer and fixed the inhomogeneous broadening for all the values of N_{lyr}. Therefore, to understand the effect of Γ_{inh} we plot the trend of J_{th} at different Γ_{inh} in Fig. 1(b). A further increase in J_{th} for the entire values of N_{lyr} is observed when Γ_{inh} increases from $15\ meV$ to $45\ meV$. This observation is relatively consistent with the results from literature that are based on Qdot model [18] since Qdashes may be thought of an elongated Qdots with quasi zero dimensional DOS. Here, we make an effort to explain this observation qualitatively in a generalized manner. Increase in J_{th} may be ascribed to the increase in size dispersion of the dashes, particularly the height, which possibly increases the internal absorptions (due to dispersion in energy states of dashes resulting in overlapping states). Higher energy photons from smaller dashes which acquire lasing conditions first (due to their dot like features) get absorbed by the longer dashes (with relatively smaller band transition energies) which eventually dominate due to their higher modal gain and DOS.

For a Qdash laser with a single stack layer, no lasing is observed experimentally and J_{th} reaches an infinite value, as depicted in Fig. 1(a). This has been attributed to the very small Γ and low dash density [5]. However, the numerical results show that besides the above mentioned parameters Γ_{inh} strongly affects the lasing condition and is an important parameter when $N_{lyr} \le 2$. In Fig. 1(b), less inhomogeneous Qdash lasers ($\Gamma_{inh} = 15$ and $25\ meV$) show lasing even for a single stacking layer and small Γ (0.009), attaining J_{th} values of 115 and $233\ A/cm^2$, respectively, unlike for $\Gamma_{inh} = 45\ meV$ which does not lase (even at $1250\ A/cm^2$). This observation may again be ascribed to reduced internal absorptions due to relatively similar energy states of dashes in the less inhomogeneous system, thus being able to attain lasing from the low density single dash layer with small Γ. Our model also predicts a minimum of J_{th} for the two and three layer stack structures irrespective of the active region inhomogeneity values. This supports the experimental observation of Fig. 1(a) and also the numerical study of the Qdots [18]. In general, based on our observation we may write a

#143370 - $15.00 USD Received 1 Mar 2011; revised 12 May 2011; accepted 17 May 2011; published 27 Jun 2011

relation for J_{th} in a similar manner reported for Qdots [16], as $J_{th} \propto \Gamma_{inh} V_A / \Gamma$, where Γ, Γ_{inh}, and V_A dominates at the two extreme values of stack number (1 and 8, respectively). However, for $N_{lyr} = 2$ and 3 these parameters probably balance each other thus attaining a relatively small value of threshold current density.

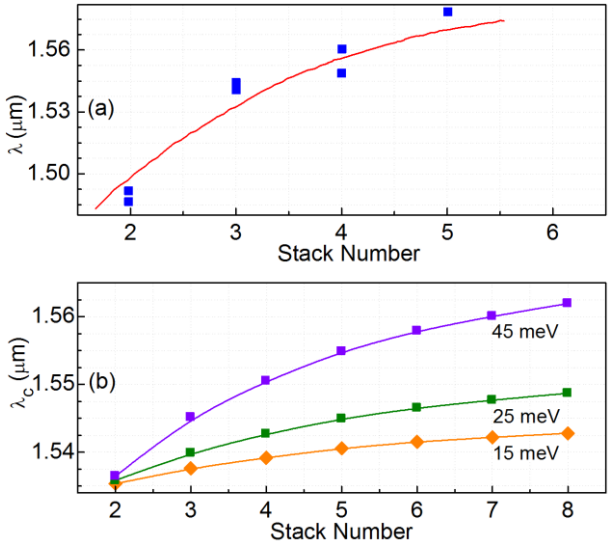

Fig. 2. (a) Experimental [5] and (b) calculated lasing wavelength as a function of the stack number for the Qdash lasers reported in [5] and [15], respectively. The three curves in (b) correspond to various inhomogeneous broadening values calculated at low current injection ($1.1J_{th}$).

The experimental results [5] of lasing spectra as a function of the stack number are shown in Fig. 2(a) and the results obtained from the model in Fig. 2(b). A red shift trend in λ_c is observed experimentally on increasing N_{lyr}, which is well reflected by our calculation, thus showing the effectiveness of our model. The behavior is seen to be consistent with increasing inhomogeneity. A total red shift of $\sim 7.5\ nm$ is observed on increasing the stack number from 2 to 8, corresponding to $\Gamma_{inh} = 15\ meV$. Since, the model does not take into consideration the growth and processing parameters that affect the lasing wavelength, we may attribute this observation to the optical confinement factor (lowers with increase in N_{lyr}) which probably assists in achieving the Γg_{th} rather early. Therefore the lasing condition might be achieved with occupation of carriers in relatively lower energy states, thereby lasing at longer wavelength. Note that the emission at shorter wavelength due to increase in J_{th} with N_{lyr} is suppressed.

Interestingly, our results show that the red shift phenomenon may also be attributed to active medium inhomogeneity. To support this statement we compare the lasing spectra of Qdash lasers at various explicit values of Γ_{inh} in Fig. 2(b). Considering $N_{lyr} = 6$ at $\Gamma_{inh} = 15\ meV$, we observe $\lambda_c = 1541.6\ nm$ and at $\Gamma_{inh} = 45\ meV$, we have $\lambda_c = 1557.9\ nm$. These values correspond to a red shift of $\sim 16.5\ nm$ when Γ_{inh} is increased three times. Moreover, a total red shift of $\sim 26\ nm$ is observed for $\Gamma_{inh} = 45\ meV$ on increasing N_{lyr} from 2 to 8, which is more than three times the value of less inhomogeneous system. This unique observation is a consequence of a quasi zero dimensional DOS of the Qdashes which exploits the increase in the higher energy tail states due to dispersion in dash sizes as a result

#143370 - $15.00 USD Received 1 Mar 2011; revised 12 May 2011; accepted 17 May 2011; published 27 Jun 2011

of increase in Γ_{inh}. In general, dispersive dash sizes result in overlapping DOS which probably increases the states in the high energy tail of the dashes DOS. Therefore, higher energy photons from shorter dashes (smaller height and larger band transition energies) which lase first probably get absorbed in the high energy tails (now incorporating more electronic states due to overlap) of longer dashes (larger height and smaller band transition energies) which lase later and eventually dominate. Therefore, lasing occurs at longer wavelengths due to the small energy photons of the longer dashes. As Γ_{inh} increases, the dashes with least band transition energy subsequently dominate and the lasing shifts to longer wavelengths (red shift of λ_c). In general, we may then deduce the relationship $\lambda_c \propto \Gamma_{inh}\Gamma$.

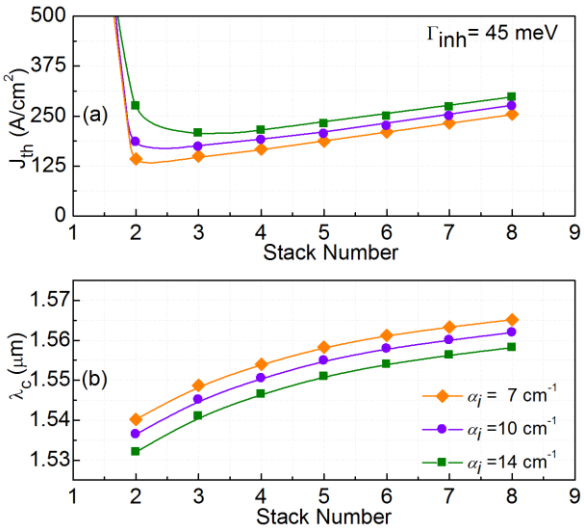

Fig. 3. Calculated (a) threshold current density and (b) central lasing wavelength (at $1.1J_{th}$) for different internal loss values for the Qdash laser reported in [15]. The inhomogeneous broadening is 45 meV.

In our earlier analysis, we have fixed the modal gain Γg_{th} irrespective of increasing N_{lyr}, although experimentally it is shown to increases with N_{lyr} [1,6,16]. Therefore, we now explore the effect of Γg_{th} by varying the internal loss α_i on the threshold current density and the central lasing wavelength as a function of N_{lyr}. The results are shown in Figs. 3(a) and (b), at fixed Γ_{inh}. We observe that lower α_i ($7\ cm^{-1}$) decreases J_{th} and enhances the red shift of λ_c for all values of N_{lyr}. This is typically the practical case for few stacks, where the lasing condition is achieved rather fast due to lower Γg_{th} ($\approx 19\ cm^{-1}$). Hence, further shift to the longer wavelengths is predicted theoretically. However, an increase of J_{th} and a reduction of red shift phenomenon is observed at large α_i ($14\ cm^{-1}$) as illustrated in Fig. 3. This is again consistent with the number of stacking layers. The observation may again be related to the practical case of a large stacking layer structure which improves the modal gain ($\Gamma g_{th} \approx 26\ cm^{-1}$) but with the expense of an increased J_{th} and a shift of λ_c to shorter wavelengths. Besides, Fig. 3(b) show that Γ_{inh} is still the dominant parameter of the red shift phenomenon.

#143370 - $15.00 USD Received 1 Mar 2011; revised 12 May 2011; accepted 17 May 2011; published 27 Jun 2011

4. Conclusion

In conclusion, we have demonstrated theoretically the effect of the number of stacking layers on the characteristics of Qdash lasers. Our model predicts an increase in threshold current density as a result of an increase in the stack number, inhomogeneous broadening and modal gain. We have shown that the red shift phenomenon is a result of the optical confinement factor and, more significantly, of the inhomogeneous broadening. We have qualitatively explained the enhanced red shift phenomenon due to the active medium inhomogeneity by considering the unique DOS of Qdashes.

Acknowledgment

The work was supported by a joint program between KAUST and the University of Michigan, Ann Arbor, under KAUST- Academic Excellence Alliance (AEA) 2010 Grant.

#143370 - $15.00 USD Received 1 Mar 2011; revised 12 May 2011; accepted 17 May 2011; published 27 Jun 2011